

Supporting Information for

Sub-20 fs All-Optical Switching in a Single Au-Clad Si Nanodisk

Gustavo Grinblat^{1}, Rodrigo Berté^{1,2}, Michael P. Nielsen^{1,3}, Yi Li¹, Rupert F. Oulton¹, Stefan A. Maier^{1,4}*

¹The Blackett Laboratory, Department of Physics, Imperial College London, London SW7 2AZ, United Kingdom

²CAPES Foundation, Ministry of Education of Brazil, Brasília, DF 70040-020, Brazil

³School of Photovoltaic and Renewable Energy Engineering, University of New South Wales, Sydney NSW 2052, Australia

⁴Chair in Hybrid Nanosystems, Nanoinstitut München, Fakultät für Physik, Ludwig-Maximilians-Universität München, 80539 München, Germany

*Corresponding author
Email: g.grinblat@imperial.ac.uk

S1. Fabrication of Au-covered Si nanodisks

A 180-nm thick amorphous Si film was sputtered on top of borosilicate glass at 0.2 \AA/s at $350 \text{ }^\circ\text{C}$, then coated with positive-tone PMMA (950K A4) resist, and post-baked at $180 \text{ }^\circ\text{C}$ for 5 min. The nanostructures were then defined by an electron beam exposure, followed by a development procedure. Cr thermal evaporation at 0.2 \AA/s to attain a 60-nm thick layer, and lift-off process in acetone were the two steps performed to obtain a metallic sacrificial mask on top of the Si film. A reactive ion etching (RIE) recipe with a mixture of SF₆ and CHF₃ was used to etch through Si and stop at the silica interface with 5% excess etching time. Cr etchant was used to remove the sacrificial hard mask and finally a layer of Au was evaporated at 2.0 \AA/s to achieve the hybrid devices. Figure S1a shows a representative scanning electron microscope (SEM) image of a selected region of the sample. The inset, together with the EDS (energy-dispersive X-ray spectroscopy) maps in Figure S1b,c, reveal the presence of only small traces of Au at Si side walls.

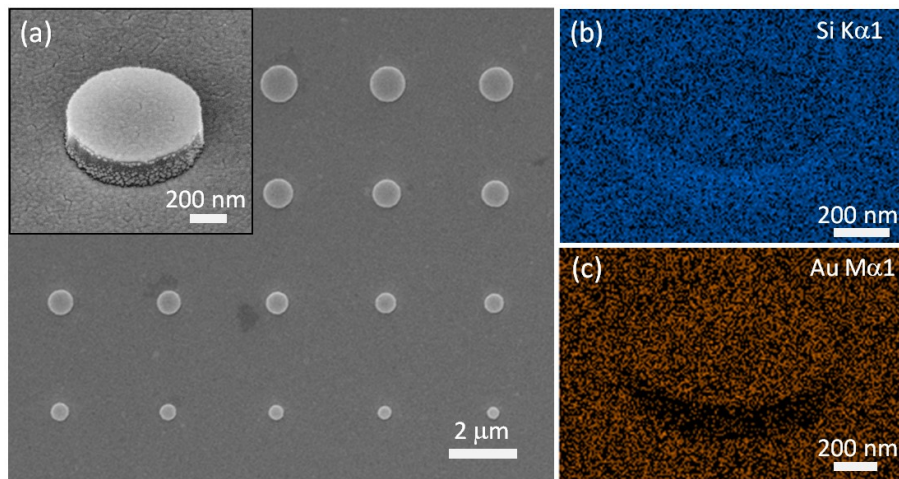


Figure S1. (a) SEM image of a portion of the fabricated sample. The distance between adjacent disks is $3 \mu\text{m}$. The inset shows an amplified image of a single nanodisk. (b,c) Corresponding EDS maps of Si (b) and Au (c) elements in the nanodisk.

S2. Linear optical characterization of nanoantennas

Dark-Field spectroscopy

The scattering spectra of single Au-covered Si nanodisks were measured by dark-field spectroscopy using a custom-built setup. Samples were mounted on a XYZ piezo stage, and illuminated at grazing incidence using a 100x, NA = 0.8 darkfield objective and a mercury lamp source (Nikon). The scattered signal from the antenna was collected via the same objective (size of collection spot ~600 nm in diameter) and directed toward a spectrograph (PI Acton SP2300 by Princeton Instruments) coupled to a CCD camera (Pixis 100B, Princeton Instruments) for the spectral characterization.

Simulations

Finite-difference time domain (FDTD) simulations of the scattering spectra of Au-covered Si nanodisks were performed with the commercial software *Lumerical FDTD Solutions*. The nanoantennas on a SiO₂ substrate were illuminated by a linearly polarized plane-wave at normal incidence. Perfectly-matched layers (PML) were used to avoid reflection at the boundaries of the simulation region. The software built-in optical properties of Au and SiO₂ were used in numerical calculations, while for the sputtered Si the optical properties employed were used as measured by ellipsometry. To compute the electric energy $W_E = \frac{1}{2} \times \iiint \epsilon(\vec{r}) |E(\vec{r})|^2 dV$ inside the Si nanodisk, monitors were placed around the Si disk to define the volume (V).

S3. Autocorrelation of pump and probe pulses

Figure S2b,c shows interferometric-FROG measurements of the pump and probe pulses (see spectrum in Figure S2a) at the position of the sample. The traces reveal pulse widths of 7.6 fs and 6.5 fs for the pump and probe beams, respectively, calculated as the FWHM of the corresponding intensity envelopes, using Prof. Trebino's FROG algorithm (<http://frog.gatech.edu/code.html>).

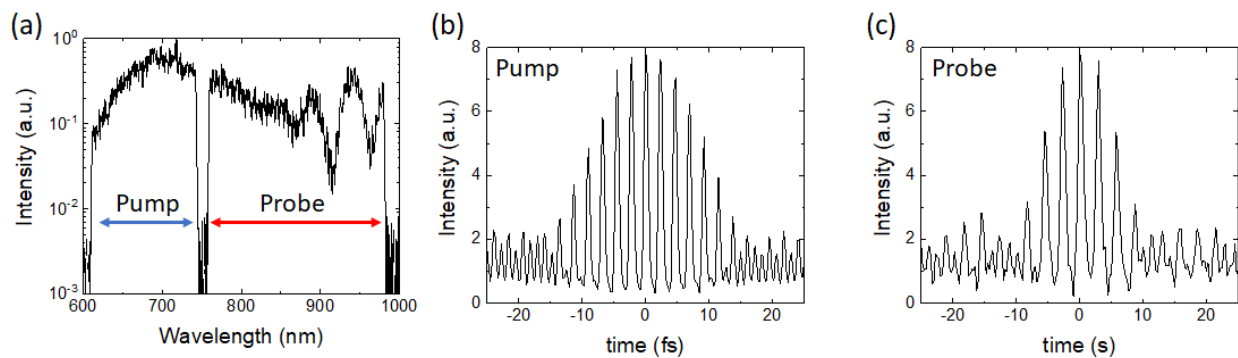


Figure S2. (a) Spectrum of pump and probe pulses. (b,c) Interferometric-FROG traces measured for the pump (b) and probe (c) pulses.

S4. Pump-probe spectroscopy in the picosecond range

Figure S3 shows differential reflectivity contour plots for representative Au-covered Si nanodisks of 630 (a) and 670 (b) nm diameters in the picosecond time range. It can be noticed that the FC contributions do not vanish even after 30 ps, in contrast to the ultrashort sub-20 fs nonlinear response highlighted with arrows in the figure.

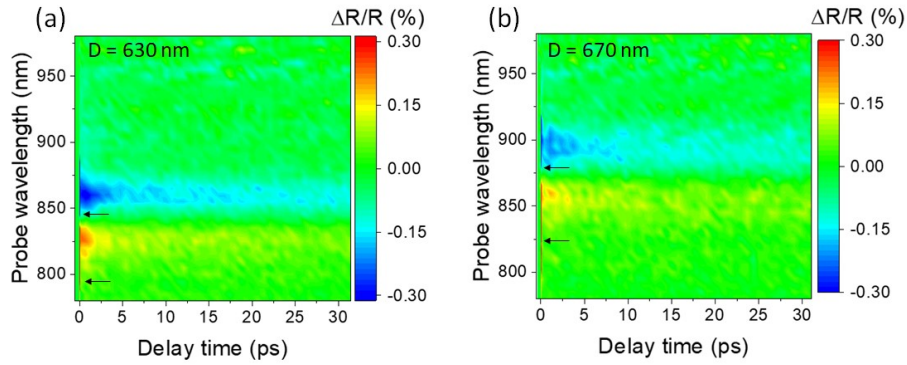


Figure S3. (a,b) Differential reflectivity spectra as a function of pump-probe delay time for single Au-covered Si nanodisks of 630 (a) and 670 (b) nm diameters. The arrows in the graphs indicate the ultrafast OKE contributions.

S5. Measurements on bare Si nanodisks and Au-film samples

Figure S4a-c shows pump-probe spectroscopy results from a bare 30-nm thick Au film (a), a single 550 nm diameter Si nanodisk (b), and a 670 nm diameter Au-covered Si nanodisk (c). The disk diameters were chosen to present the ultrafast nonlinear response in the same wavelength region. Results show that the metallic film exhibits negligible signal compared to that of the nanoantennas, suggesting that the observed response originates mainly from the dielectric element. Indeed, the bare Si nanodisk shows a similar behavior to that of the Au-covered case, but with much lower signal-to-noise ratio. It should be noticed that the response of the all-dielectric antenna deteriorates when performing several consecutive measurements, possibly due to the absence of the metallic layer, which allows efficient heat dissipation for the hybrid nanodisk.

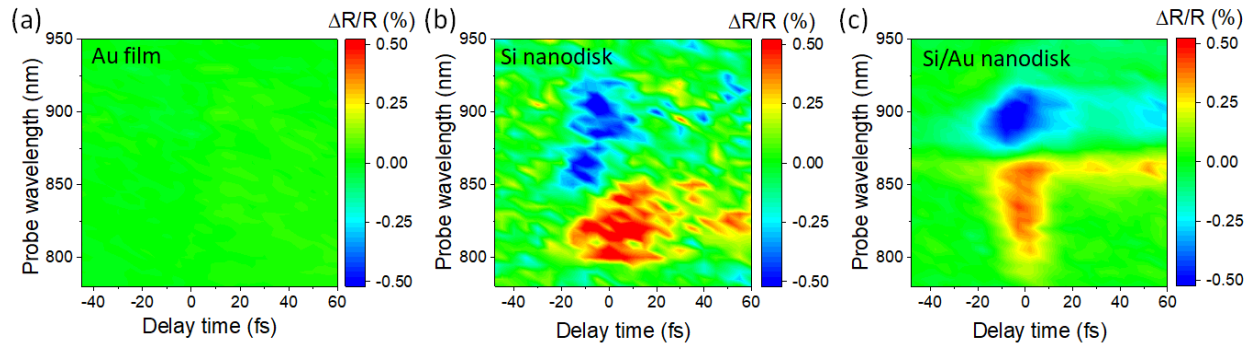


Figure S4. (a-c) Differential reflectivity measurements of a 30 nm-thick Au film (a), a 550 nm diameter Si nanodisk (b), and a Au-covered Si nanodisk of 670 nm diameter (c).